Available online at www.sciencedirect.com

ScienceDirect

Procedia Engineering 103 (2015) 341 – 348

Procedia Engineering

www.elsevier.com/locate/procedia

The 13th Hypervelocity Impact Symposium

Investigations of High Performance Fiberglass Impact Using a Combustionless Two-Stage Light-Gas Gun

Leslie Lamberson[a]*

[a]Drexel University, 3141 Chestnut Street, Philadelphia, Pennsylvania, 19104, USA

Abstract

Two types of high performance fiberglass panels were investigated at normal impact conditions of around 1 km/s (2200 mph). Thin phenolic laminates of plain-weave glass cloth impregnated with synthetic thermosetting resins, one melamine and the other epoxy, were impacted by a 1.6 mm diameter nylon sphere using a combustionless two-stage light-gas gun. The resulting impact and ejecta was captured using high-speed imaging, and the perforation characteristics and damage zone were examined post-mortem using optical microscopy. Both composites had a fiber volume fraction of an estimated 56% and identical fiber weave so that the role of the matrix on impact performance could be comparatively investigated. The epoxy fiberglass resulted in full perforation of the target, whereas the melamine fiberglass resulted in deformation, but not full perforation. The overall damage zone of melamine fiberglass was twice the size on the rear surface than the epoxy fiberglass. In addition, the melamine fiberglass rear damage zone was 5 times the impactor diameter and exhibited ductile debonding and delamination as the main failure mechanisms. In contrast, the epoxy matrix rear damage was 3 times the impactor diameter and exhibited brittle failure mechanisms of fiber breakage and pullout. These experimental results suggest that the matrix material is a driving factor in the impact damage and perforation characteristics, and is discussed in context of the compressive and tensile strength at break of the materials.

Peer-review under responsibility of the Curators of the University of Missouri On behalf of the Missouri University of Science and Technology

Keywords: fiberglass, perforation, fiber breakage, debonding, impact resistance

Nomenclature

D_F	front surface damage diameter (mm)
D_R	rear surface damage diameter (mm)
D	cavern diameter (mm)

1. Introduction

High performance fiberglass materials are being increasingly used in aerospace applications due to their favorable mechanical properties and reduction in weight over traditional metals. However, two main concerns in the use of advanced composites is the lack of study on the translaminar properties and fiber-matrix interface that are critical to impact loading resistance [1-3]. Consequently, a fundamental understanding of the damage and failure mechanisms at the ply-interface as

* Leslie Lamberson Tel.: +1-215-571-3519; fax: +1-215-895-1478.
E-mail address: les@drexel.edu.

Peer-review under responsibility of the Curators of the University of Missouri On behalf of the Missouri University of Science and Technology
doi:10.1016/j.proeng.2015.04.056

well as the constituent-interface, and its role in translaminar damage and interface adhesion is imperative in achieving their widespread use.

This paper presents a novel combustionless two-stage light-gas gun and uses it to examine two types of high performance fiberglass materials. Both fiberglass sheets have a plain-weave cross-ply structure with continuous glass filaments. One has a melamine thermosetting resin and the other epoxy with commercial names of Garolite G-9 and G-10, respectively. While their nominal layup is the same, the performance at 1 km/s normal impact revealed strikingly different results. The resistance to perforation appeared to improve with the fiberglass exhibiting higher matrix tensile strength at break perpendicular to the weave and slightly higher dynamic compressive strength. Unlike the epoxy fiberglass that exhibited fiber breakage and pullout as its dominant failure mechanisms, the more penetration-resistant melamine fiberglass exhibited large zones of debonding and delamination. In this regard, the composite acted like a net that spread the impact energy to a larger damage zone, allowing the plys to debond and flex to absorb energy, and preventing complete perforation of the impactor in the process.

1.1. Background

A large amount of impact literature on woven fiberglass phenolic resin composites focuses on layering the sheets with other materials such as Kevlar or aluminum at low impact speeds. For example, Atas examined fiberglass-aluminum composites (epoxy resin) under drop tower impact conditions and showed an increase in impact damage zone and delamination with increasing impact energy from 5 to 70 J [4]. Salehi-Kojin et al. examined Kevlar-fiberglass (epoxy resin) composites at low velocity impact energies of 8 to 25 J and considered temperatures of -50 to 120^0C. They found that maximum panel deflection increased from 0 to 120^0C, and decreased from -25 to 0^0C [5]. Gupta and Davids examined a fiberglass reinforced polyester resin sheets 0.09 to 0.25 in thick impacted at 387 m/s and found that the weight efficiency of the fiberglass cloth was greater than that of steel [6].

Under high strain-rate compressive uniaxial conditions, Garolite G-10 has been examined using a Kolsky or split-Hopkinson bar at 10^2 and 10^3 s^{-1}. Nishida et al. examined three strain-rates (270, 500, and 1000 s^{-1}) in both the in-plane and out-of-plane loading configurations with respect to the laminate plys. They determined that the material did not appear to be rate sensitive in either its strength or failure properties [7]. Ravi-Chandar and Satapathy examined the same G-10 composite in quasi-static and dynamic uniaxial compression. They observed some nonlinear rate dependence attributed to the polymer matrix and showed at least a two-fold increase in compressive strength from quasi-static to dynamic compression, as well as cracking at a 45 degree angle from the loading direction [8]. Lamberson et al. examined both G-9 and G-11 Garolite fiberglass (melamine and epoxy resins, respectively), where G-11 is similar to G-10 except it has resin additives to increase its insulative properties and high temperature resistance. Under quasi-static and dynamic compressive conditions, they found that the melamine matrix composite exhibited rate dependency from 10^{-3} to 2400 and 4500 s^{-1}, reaching twice the quasi-static compressive strength at the highest strain rate; whereas the epoxy resin reached 1.7 times it's quasi-static compressive strength the highest strain-rate tested of 3800 s^{-1}. They also noted that both materials exhibited matrix cracking with the formation of shear type bands at around 45 degree angles formed during quasi-static and dynamic deformation [9].

At hypervelocity speeds (> 3 km/s) Silvestrov et al. examined glass reinforced epoxy laminated composites normally impacted at 8 to 11 km/s by steel and glass projectiles of 0.53 to 4.5 mm diameters using a tubular high explosive accelerator [10]. The resulting perforation characteristics of the 5 cm thick plates of a strawglass weave (50% fiber volume fraction) with epoxy resin plys 0.1 to 0.3 mm thick were examined using a Charters-Summers formula showing a linear increase in the ratio of density and perforation diameter with impact speed. A broad review of the crater formation and delamination of various fiber-reinforced, cured resins and epoxy composites impacted from 3.5 to 9 km/s at the NASA Ames vertical gun facility is presented by Cour-Palais [11]. Schonberg examined graphite-epoxy composite systems under hypervelocity impact and noted that the rear side spall decreased for these systems when compared to aluminum shield systems [12]. Tennyson and Lamontagne examined graphite/PEEK laminates at 2 to 7 km/s and observed both material damage and ejecta plumes, determining the debris plume particles have sufficient energy to penetrate adjacent structures and cause major secondary structural damage [13]. Lamontagne et al. also examined carbon/PEEK composites for normal and oblique impact performance at 5 km/s, and found that for a given impact energy, the damage area in the 24 ply targets was nearly twice that of the 16 ply targets [14]. While the studies mentioned do not cover the expansive amount of research conducted on the impact performance of fiberglass and graphite composites, it illustrates the nature of the variability in material constituents, test configurations, and overall performance.

The present study focuses on glass fiber polymer matrix composites that have nonlinear, rate-dependent and viscoelastic behavior. This study also examines impact speeds between those generated from low-velocity launchers (such as drop-tower tests) and those from large-scale hypervelocity impact facilities where velocities exceed 3 km/s.

2. Experimental Configuration

2.1. Combustionless Two-Stage Light-Gas Gun

A novel combustionless two-stage light-gas gun was developed and built at Drexel University in the Dynamic Multifuctional Materials Laboratory to span high-speed to hypervelocity impact ranging from approximately 1 to 3 km/s. Completed in 2014 and shown in Figure 1, the facility utilizes a smooth bore design. The unique aspects of the facility is in the first stage, or Stage 1. The driving section of Stage 1 uses 700 kPa (100 psi) of compressed air to initiate the 1 km/s and greater impacts instead of combustion initiation (explosion) and is designed for easy separation and use as a single-stage gun by itself. This pressure differential design uses compressed air to launch a piston forward, compressing helium through the second stage (or Stage 2), launching a projectile into a target chamber held in vacuum. The overall facility is less than 3 meters in total length and has an expendable cost per shot that is one to two orders of magnitude lower than more traditional two-stage light-gas gun facilities.

The first stage consists of a 0.75 m long, 0.5 m diameter barrel which houses a smaller barrel inside with a 1.27 cm inner diameter. A HDPE piston 1.27 cm diameter and 5 cm long is held by a small amount of vacuum at the uprange end of the inner barrel where it seals slots that expose the outer barrel. The portion of the inner barrel downrange of the piston is brought to vacuum and filled with helium gas. The outer barrel is filled with compressed air and when the uprange vacuum holding the piston is released, the piston is nudged forward and exposes the slots from the outer barrel. The air then rushes behind the piston and pushes it down the barrel. Thus, the only moving part of the first stage is the piston itself.

At the uprange end of the barrel, the piston is stopped nondestructively by a sacrificial rubber nose cone, and the hydrogen gas is compressed through an area reservoir section (AR) that is the shape of a converging nozzle to further accelerate the flow. At the downrange end of the AR section, a 0.35 mm thick Mylar burst disc is separating the hydrogen from a 0.3 mm steel flight tube that houses the impactor. From the build up of the hydrogen, the Mylar burst disc breaks and releases the nylon 6/6 1.6 mm diameter sphere down the flight tube and into the target chamber, all of which is under vacuum. The target chamber is 1.3 meters in total length and has 3 optical ports for visualization, one diagnostic port and one large rear door for the target rig. High-speed imaging from a Photron SA-5 with a 105 mm lens was utilized outside the tank at 50,000 frames per second (fps). Two 6V krypton bulb lights providing a total of 150 lumens of light was placed inside the tank directly under the shot line, in order to configure a shadowgraph method to visualize impact characteristics.

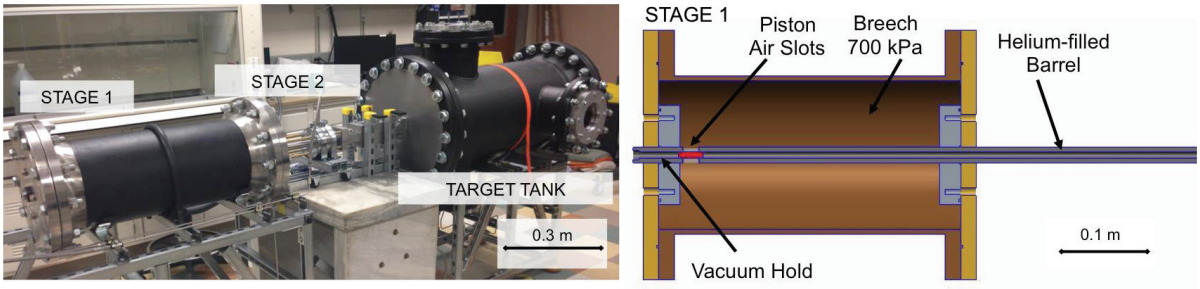

Fig. 1. (Left) Pressure-Differential Hypervelocity Impact Facility (PHIR) at Drexel University. (Right) Cut-away engineering drawing of Stage 1 showing pressure differential approach where piston is the only moving part that initiates 1 km/s impact using 700 kPa of compressed air as driving gas.

2.2. Fiberglass Material

Two types of commercially available fiberglass, phenolic laminates of plain-weave glass cloth impregnated with synthetic thermosetting resins of melamine and epoxy known as Garolite 9 and 10, were studied. Each had an estimated fiber volume fraction of 56% and similar densities. Their microstructure is shown in Figure 2.

The composite samples used for testing were 0.8 mm thick and 150 by 150 mm. The samples were mounted in aluminum frames, providing a pinned boundary condition on all sides, and mounted on optical posts. The impact direction was aligned by means of an optical breadboard and rail centered inside the target tank. The impacts were configured to occur normal to the ply layup direction, and a 9.5 mm thick witness plate of steel was set up approximately 150 mm behind the target as a full-stop. Table 1 lists relevant material properties of these samples.

Melamine alone has a compressive strength under quasi-static conditions of 196 MPa, and epoxy of 178 MPa [15]. Melamine resin is made of melamine formaldehyde, a thermosetting plastic with cross-linked nitrogen bonds that bind the material together; whereas the epoxy resins, also known as polyepoxides, have cross-linked epoxide groups that lack ester groups within the molecular chain [16]. The complex bonding in the polymers helps give them their strength.

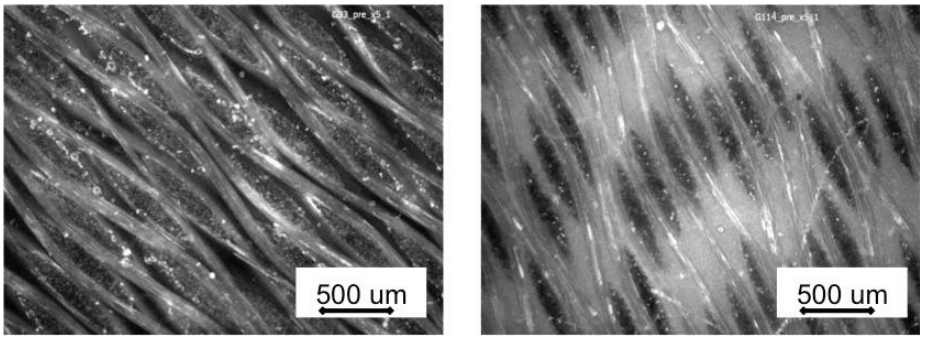

Fig. 2. (Left) Melamine matrix fiberglass (Right) Epoxy matrix fiberglass microstructure illustrating plain-weave weft and warp fiber scale and density.

Table 1. Relevant properties of plain-weave cross-ply fiberglass materials used in the study, * [9] **crosswise [15].

Type	Volume Fiber Fracture	Matrix	Density (kg/m^3)	Compressive Strength* (MPa)	Tensile Strength at Break** (MPa)
Garolite G-9	54%	Melamine	1850	484	425
Garolite G-10	54%	Epoxy	1800	381	262

3. Results and Discussion

3.1. High-Speed Impact Results

A summary of the test results can be found in Table 2 for impact velocities of approximately 800 to 1300 km/s (1800 – 2800 mph). In the case of the epoxy fiberglass, the impacts resulted in full perforation of the targets. Shot N11 of the epoxy fiberglass resulted in forward and rear ejecta as the impactor continued downrange. Shot N12 epoxy fiberglass also achieved full perforation of the target, however the impactor rebounded off the front of the target and no discernable rearward ejecta was seen. On the melamine fiberglass composites, the impact resulted in large deformation zones, but no full perforation. The fiberglass had projectile rebound velocities of 23 m/s (+/- 2.3 m/s), which could suggest that it is independent of the failure mechanisms. At the same time, it is important to note that the error associated with the ejecta speed calculations is significant (on the order of 20%) since the phenomena is a three-dimensional expansion and the images only capture a two-dimensional view at relatively low spatial resolution.

Table 2. Summary of test results of nylon 6/6 1.6 mm diameter sphere normally impacting fiberglass plates of 0.8 mm thick.

Test ID	Matrix	Impact Velocity [m/s]	Rebound Velocity [m/s]	Front Ejecta Speed [m/s]	Rear Ejecta Speed [m/s]
N11	Epoxy	1200	-	196	60
N12	Epoxy	1250	23	54	-
N13	Melamine	1000	25	157	-
N14	Melamine	780	21	24	-

An example of the shadowgraph results is shown in Figure 3 for a melamine fiberglass sample. The ‘Original’ image shows two 6V kypton bulb light sources illuminating the filed of view from below. The field of view was approximately 200 mm by 100 mm, and the framing rate was 50,000 fps. A MATLAB code using image toolbox was written to post-process the images by subtracting the original image from all subsequent images to help visualize the projectile and improve

contrast of the impact response. Due to the slow interframe time of the camera, taking an image every 20 microseconds, combined with the high speed of the projectile, the projectile appears streaked in the images as it travels to the target downrange. The relative velocity was calculated with respect to the impactor position in each frame, as well as by the known distance remaining to the target, and the measurements had an average standard error (of the mean) of 16.8% (178 m/s). Light catches the ejecta, and the slower-moving bright spot is the rebounded impactor traveling back uprange. There appears to be little to no dwell time between initial impact and rebound.

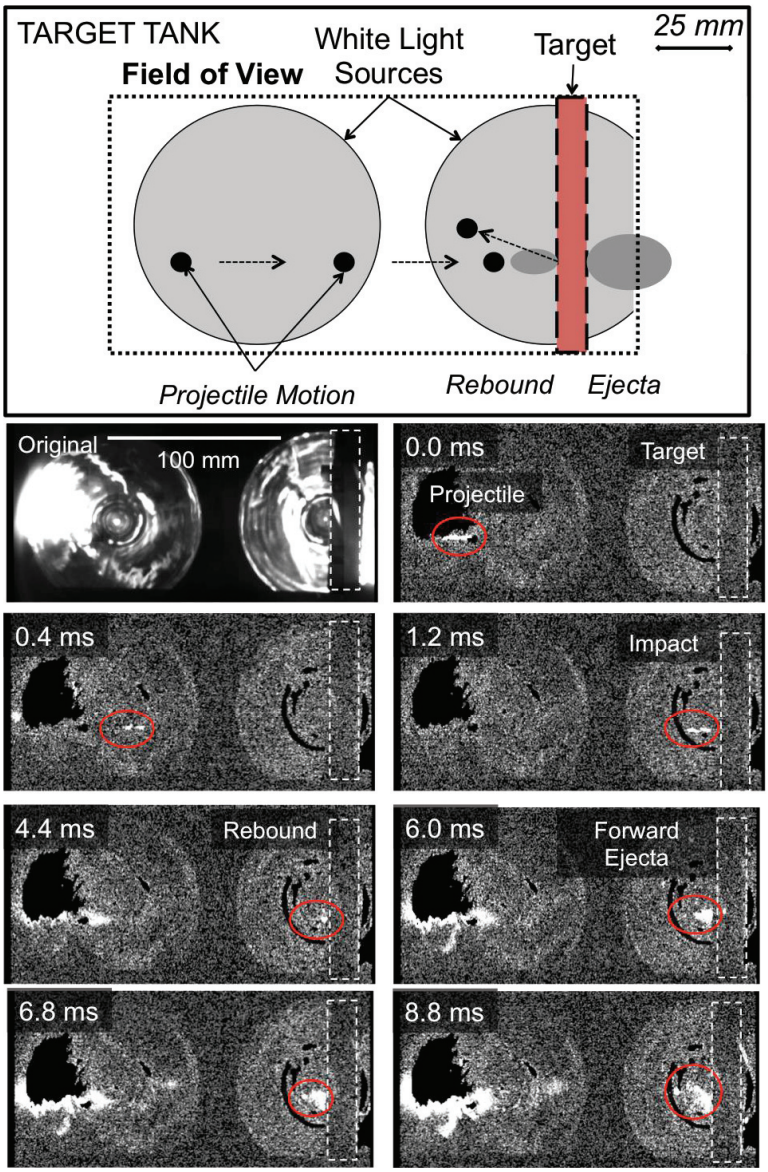

Fig. 3. (Top) Schematic of filed of field of impact tests. (Bottom) Shadowgraph images of high-speed impact event of nylon sphere 1.6 mm diameter impacting a 0.8 mm thick melamine fiberglass target at 780 m/s. The 'Original' image shows an unprocessed image of the event before the projectile enters the field of view with the target outlined in white dashed marks on the right side. The subsequent images have been post-processed in MATLAB, subtracting out the original image to only view the changes in light. The next 1.2 ms show the projectile traveling from the left to the right and is circled in red. The impact happens after 1.2 ms and then the forward ejecta appears, meanwhile the rebound of the projectile is already well underway. At 6.8 and 8.8 ms the bright spot is the impactor traveling back uprange (circled in red) with ejecta visible from the target surface.

3.2. Post-Mortem Microscopy

A table with the resulting damage length scales for each test is shown in Table 3 with a schematic in Figure 4. Figure 5 illustrates the impact zones on the front and back of the two composites studied. The maximum length of the damaged region, i.e. the largest diameter of the visible impact zone on the front and rear surface labeled D_F and D_R, was taken by averaging at least three measurements using ImageJ. In the case of full perforation, a cavern diameter was also taken, D. Results indicate that on the downrange surface, the melamine fiberglass had much larger damage zones than the perforated epoxy fiberglass, or 5 times the diameter of the projectile. The epoxy fiberglass had a damage zone approximately 3 times the diameter of the projectile, and the cavern diameter was essentially the same size or slightly smaller than the projectile diameter.

Table 3. Summary of test results of nylon 6-6 1.6 mm diameter sphere normally impacting fiberglass plates of 0.8 mm thick.

Test ID	Matrix	Max Front Damage Zone D_F *(mm)*	Ratio of D_F / Projectile Diameter	Max Rear Damage Zone D_R *(mm)*	Ratio of D_R / Projectile Diameter	Cavern Diameter *D (mm)*
N11	Epoxy	4.5	2.9	5.7	3.6	1.2
N12	Epoxy	6.5	4.1	6.0	3.8	1.6
N13	Melamine	9.7	6.1	15.3	9.7	-
N14	Melamine	7.2	4.6	9.3	5.9	-

Images of the post-mortem impact surfaces clearly show perforation in the epoxy fiberglass samples, and larger damage zones in the melamine fiberglass (Figure 5). It appears that while the incoming kinetic energy was nominally the same for the impacts, the epoxy fiberglass exhibited significant fiber breakage and the melamine fiberglass exhibited significant debonding and delamination to absorb the energy.

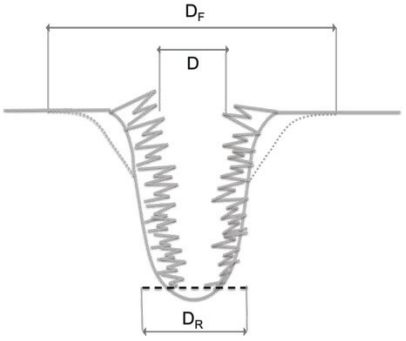

Figure 4: Qualitative sketch of damage through the thickness of composite where D_F is the total front surface damage diameter which has a 'whitening' zone, D_R is the rear surface damage diameter (which may have full perforation or hole along with a whitening region of damaged material), and D is the cavern diameter or the length of the full perforation form the front side of the target. The lighter lines on the side of the damage zone show the whitening region that is visible from the surface. Figure adapted from [10].

The performance difference between the two materials could be due to the fact that impact damage depends significantly on the material strength in both tension and compression. The melamine fiberglass is twice as strong in tensile strength at break in the crosswise direction than the epoxy fiberglass. The two fiberglass materials have closer comparative compressive strengths. When the impactor strikes, the matrix material on the surface cracks and is ejected away from the composite. Given that the projectile incoming kinetic energy density far exceeds the material strength, and the layers begin to deform in compression. The resulting deformation can either be brittle or ductile in nature given the constituent materials, bonding, and adhesion properties, which leads to a competition of failure mechanisms that convert incoming energy to work done on the target. As the impactor is decelerating while compressing the target, stress waves propagate and interact across the boundaries. At this point the material begins to either crack (brittle) and/or to bend and stretch to accommodate the dissipation of energy (ductile). While the impact itself is characterized as a compressive load, the stretching of the fabric can reach a tensile mode on the rear surface of the plate to accommodate energy dissipation. For the epoxy fiberglass, the material is weaker in tension, leading to fiber fracture before significant stretch in the material is achieved. This is ly

localized mechanism, and forms a cavern zone in the target so that full perforation is achieved. For the melamine fiberglass, the fabric composite is able to deform and flex via plastic-like response, debonding and delaminating to develop a large whitening zone. These mechanisms are less localized, allowing for kinetic energy to be dissipated over a larger area.

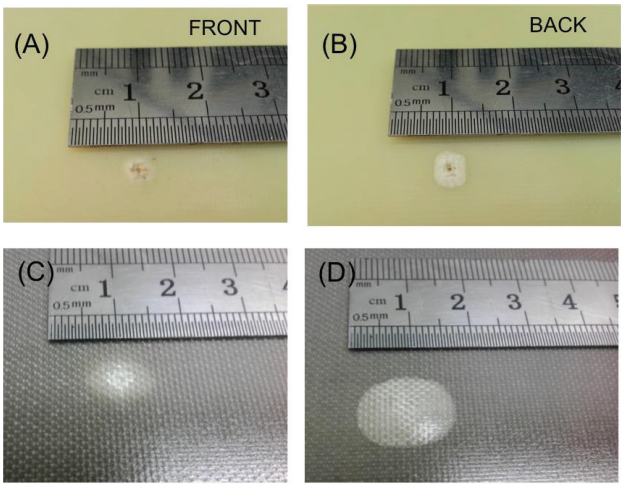

Figure 5: (A) Front surface of impacted epoxy fiberglass. (B) Rear surface of impacted epoxy fiberglass with full perforation visible. (C) Front surface of melamine fiberglass with no discernable cavern diameter and a large whitening region. (D) Rear surface of impacted melamine fiberglass with large damage whitening zone.

When the samples were examined under an optical microscope, both fiberglass composites exhibited matrix cracking that grew parallel and perpendicular or along the weft or warf directions of the weave. The matrix cracking was visible mainly on the back of the sample, as the front surface matrix material had been ejected on impact. The melamine exhibited a radial type cracking that was not as noticeable in the epoxy fiberglass on both the forward and rear surfaces. Visible cracks would grow at angles from the weft/warf directions. Fiber breakage in the cavern diameter is clearly present in the epoxy fiberglass. These failure mechanisms are shown in Figure 6 below.

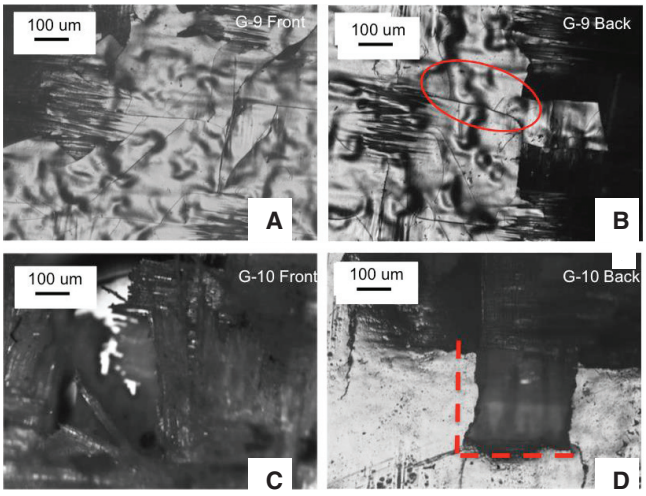

Figure 6: The top two figures show matrix cracking at angles other than the weft or warf weave directions on both the front (A) and back (B) surfaces of the melamine fiberglass (circled in red on the rear surface image). The light color material is the matrix and the dark is the fibers. The bottom two images show the front (C) and back (D) of the epoxy fiberglass impacted surfaces. Clear perforation is shown on the front surface with visible fiber breakage in the through thickness of the front surface with light showing through (C), whereas a tearing along the weft/warf (dashed in red lines) with some cracking of the matrix is shown on the rear surface (D).

4. Summary

A combustionlesss two-stage light-gas gun was used to examine two types of high performance fiberglass composites under 1 km/s normal impacts (2200 mph). Each material consisted of a plain-weave cross-ply structure with continuous glass filaments that differed in their thermosetting resins. One had an epoxy resin, and the other had melamine. While their nominal ply layup, thickness, and impact conditions were the same, the damage and perforation characteristics under impact revealed strikingly different results. The epoxy fiberglass reached full perforation with fiber breakage and pull-out, and the melamine fiberglass had a much larger damage showing debonding and delamination, but no perforation. The difference in results could be due to the difference in the tensile strength at break of the materials, where as the impact process occurs, the material that can bend and flex more before breaking to resist perforation, acts like a net, and actually dissipates energy more effectively than a localized fiber fracture response. These results provide preliminary insight towards the role the matrix in the damage resistance of high performance fiberglass.

Acknowledgements

The author would like to thank Dr. Philipp Boettcher, and students Sam Kantor, Peter Jewell, Logan Shannahan, Steven Pagano, Ryan Beck, Dominic Sciulli, Libu Geevarghese, Benjamin Wright-Rowan, Daniel Salvatore, John Barbar, Andrew Canosa, Brenden O'Brien, and Connor Whaland for their assistance in developing the gas gun and running tests. This work was supported in part by the Harry C. Bartels Endowed Faculty Engineering Development Fund through Drexel University.

References

[1] A. Mouritz, K. Leong, I. Herszberg, A review of the effect of stitching on the in-plane mechanical properties of fibre-reinforced polymer composites, Composites Part A: applied science and manufacturing, 28 (1997) 979-991.
[2] J. López-Puente, R. Zaera, C. Navarro, Experimental and numerical analysis of normal and oblique ballistic impacts on thin carbon/epoxy woven laminates, Composites Part A: applied science and manufacturing, 39 (2008) 374-387.
[3] M. Hosur, U. Vaidya, C. Ulven, S. Jeelani, Performance of stitched/unstitched woven carbon/epoxy composites under high velocity impact loading, Composite Structures, 64 (2004) 455-466.
[4] C. Atas, An experimental investigation on the impact response of fiberglass/aluminum composites, Journal of Reinforced Plastics and Composites, (2007).
[5] A. Salehi-Khojin, R. Bashirzadeh, M. Mahinfalah, R. Nakhaei-Jazar, The role of temperature on impact properties of Kevlar/fiberglass composite laminates, Composites Part B: Engineering, 37 (2006) 593-602.
[6] B. Gupta, N. Davids, Penetration experiments with fiberglass-reinforced plastics, Experimental Mechanics, 6 (1966) 445-450.
[7] E.E. Nishida, J.T. Foster, P.E. Briseno, Constant strain rate testing of a G10 laminate composite through optimized Kolsky bar pulse shaping techniques, Journal of Composite Materials, (2012) 0021998312460263.
[8] K. Ravi-Chandar, S. Satapathy, Mechanical properties of G-10 glass-epoxy composite, Defense Technical Information Center, 2007.
[9] L. Lamberson, L. Shannahan, S. Pagano, Shear Band Evolution of Fiberglass Composites in Compression, Experimental Mechanics, (2014) in review.
[10] V. Silvestrov, A. Plastinin, N. Gorshkov, Hypervelocity impact on laminate composite panels, International journal of impact engineering, 17 (1995) 751-762.
[11] B.G. Cour-Palais, Hypervelocity impact in metals, glass and composites, International Journal of Impact Engineering, 5 (1987) 221-237.
[12] W.P. Schonberg, Hypervelocity impact response of spaced composite material structures, International Journal of Impact Engineering, 10 (1990) 509-523.
[13] R. Tennyson, C. Lamontagne, Hypervelocity impact damage to composites, Composites Part A: Applied Science and Manufacturing, 31 (2000) 785-794.
[14] C.G. Lamontagne, G.N. Manuelpillai, J.H. Kerr, E.A. Taylor, R.C. Tennyson, M.J. Burchell, Projectile density, impact angle and energy effects on hypervelocity impact damage to carbon fibre/peek composites, International journal of impact engineering, 26 (2001) 381-398.
[15] L. MatWeb, MatWeb: Material Property Data, in, 2012.
[16] S.-J. Park, M.-K. Seo, Interface science and composites, Academic Press, 2011.